Reproductive Biology 23 (2023) 100818

Contents lists available at ScienceDirect

Reproductive Biology

journal homepage: www.journals.elsevier.com/reproductive-biology

Biomolecular composition of porcine ovarian follicles following *in vitro* treatment of vitamin D_3 and insulin alone or in combination

Kinga Kamińska [a,b], Ewelina Wiercigroch [c], Kamilla Małek [c], Małgorzata Grzesiak [b,*]

[a] Doctoral School of Exact and Natural Sciences, Jagiellonian University, Poland
[b] Department of Endocrinology, Institute of Zoology and Biomedical Research, Faculty of Biology, Jagiellonian University, Gronostajowa 9, 30-387 Krakow, Poland
[c] Department of Chemical Physics, Faculty of Chemistry, Jagiellonian University, Gronostajowa 2, 30-387 Krakow, Poland

ARTICLE INFO

Keywords:
FTIR
Vitamin D_3
Insulin
Ovary
Pig

ABSTRACT

The study aimed to analyze changes in biomolecular composition of granulosa and theca interna cells of porcine ovarian follicles following *in vitro* treatment of vitamin D_3 and insulin alone or in combination. Medium antral follicles (n = 4/each group) were cultured alone (C; control) or in the presence of 1α,25$(OH)_2D_3$ (VD; 100 ng/mL) and insulin (I; 10 ng/mL) separately or in combination, VD and I (VD+I). Then paraplast-embedded ovarian follicles were used for Fourier Transform Infrared (FTIR) spectroscopy and respective histological stainings. FTIR analysis revealed changes in the content of fibrous proteins (mainly collagens) within theca interna following vitamin D_3 and insulin co-administration that was verified by Masson's trichrome staining. Treatment-dependent differences were also observed in the secondary structure of proteins, indicating enhanced conversion to α-helices in response to vitamin D_3 and insulin action/interaction in both follicular compartments. In the granulosa and theca interna layers, tendency to lower DNA content in the VD+I group was noted and confirmed by Fulgen's staining. Finally, altered monosaccharides production in both follicular layers was found. Based on FTIR results, it is possible to attribute the observed alterations to biological processes that could be regulated by vitamin D_3 and insulin in the porcine ovarian follicles.

1. Introduction

Vitamin D_3 has been increasingly recognized as an vital regulatory factor within the ovary [1]. Acting through cognate nuclear and/or membranous receptors, vitamin D_3 was found to influence follicular cell proliferation and differentiation, and thereby follicle growth, development, and oocyte maturation [2,3]. Recent studies have also confirmed its modulatory effect on ovarian steroidogenesis, particularly estradiol biosynthesis [4,5]. Furthermore, both the expression of vitamin D_3 metabolizing enzymes and the presence of biologically active form of vitamin D_3 (calcitriol; 1α,25$(OH)_2D_3$) in the follicular fluid [6], additionally support its relevance in the ovarian function.

In the last years, vitamin D_3 deficiency has been recognized as a global health issue [7]. Consequently, there is a growing interest in the relationship between low vitamin D_3 status and the incidence of various diseases, including female reproductive disorders [1,8,9]. Among them special attention is paid to polycystic ovary syndrome (PCOS), a common endocrinopathy of reproductive age women characterized by reproductive, hormonal and metabolic disturbances such as insulin resistance and hyperinsulinemia [10]. Noteworthy, diminished peripheral vitamin D_3 level was predominantly found in PCOS patients [11], as well as disrupted vitamin D_3 metabolism and reduced 1α,25$(OH)_2D_3$ content was observed in ovarian tissue of rat PCOS model [12]. It is proposed that vitamin D_3 has the ability to improve insulin sensitivity, which affects not only adipose tissue or muscles of PCOS women, but also the ovary [10]. However there is a lack of data describing the interaction between vitamin D_3 and insulin at the ovary level and its biomolecular hallmarks are worth of elucidation.

Fourier Transform Infrared (FTIR) spectroscopy is widely applied to demonstrate changes in biochemical components such as proteins, nucleic acids, carbohydrates and lipids in many tissues, represented in the specific infrared (IR) spectra of absorption [13]. Recently, FTIR has been presented as a promising tool for cancer diagnosis and monitoring of tumor development that allow to simple identify novel cancer biomarkers [14–17]. So far, the ovary has been poorly examined using FTIR technique. Limited research conducted on ovarian cancer cell lines/malignant tissue showed differences in the amount of lipids and nucleic acids, as well as altered protein conformation in comparison to

* Corresponding author.
E-mail address: m.e.grzesiak@uj.edu.pl (M. Grzesiak).

https://doi.org/10.1016/j.repbio.2023.100818
Received 24 August 2023; Received in revised form 12 October 2023; Accepted 14 October 2023
Available online 18 October 2023

normal ovarian cells/tissue, providing the characteristics of various types of ovarian cancer [18].

Taking into account that the mechanism of interaction between vitamin D_3 and insulin within the ovary is weakly understood, the comprehensive approach for recognition of differences in ovarian follicle molecular content seems to be relevant and could provide new markers for identification of induced changes. Noteworthy, the pig is actually the most common large laboratory animal species. Due to many similarities in structure and function to humans, including size, anatomy and physiology, it is a relevant model organisms for biomedical research, providing a fundamental research platform for studying female reproductive endocrinology [19,20]. Thus, the aim of the study was to employ for the first time FTIR, a non-destructive and label-free technique, to indicate biochemical alterations within granulosa and theca interna layers of ovarian follicle following *in vitro* treatment of vitamin D_3 and insulin alone or in combination, using pig as a model. Furthermore, hematoxylin and eosin, TUNEL, Fulgen's and Masson's trichrome staining with quantitative analyses were conducted to confirm FTIR results.

2. Materials and methods

2.1. Reagents

Medium M199 (cat. no. M4530), antibiotic–antimycotic solution (AAS 100×, cat. no. A5955), fetal bovine serum (FBS, heat inactivated, cat. no. F9665), calcitriol (1α,25$(OH)_2D_3$; cat. no. PHR1237), insulin (cat. no. I5523), paraplast (cat. no. P3683), 3′3′-aminopropyl-triethoxysaline (cat. no. 281778), eosin Y-solution 0.5 % alcoholic (cat. no. 1024390500), dibutylphthalate polystyrene xylene (DPX; cat. no. 06522) and Schiff's reagent (cat. no. S5133) were obtained from Sigma-Aldrich (St. Louis, MO, USA). Phosphate-buffered saline (PBS, cat.no. 14040–117) was purchased from Thermo Fisher Scientific (Wilmington, DE, USA). Falcon Organ Culture Dishes (cat. no. 08–772–12) were obtained from Fisher Scientific (Schwerte, Germany). Hematoxylin QS (cat. no. H-3404) was obtained from Vector Laboratories Inc. (Burlingame CA, USA). ApopTag Plus Peroxidase In Situ Apoptosis Detection Kit (cat. no. S7101) was purchased from Chemicon International (Melbourne, Australia).

2.2. Animals and tissue collection

The use of animals was in accordance with the Act of January 15 2015 on the Protection of Animals Used for Scientific or Educational Purposes and Directive 2010/63/EU of the European Parliament and the Council of September 22 2010 on the protection of animals used for scientific purposes.

Porcine ovaries were purchased from healthy, mature cross-bred gilts (Large White × Polish Landrace; ~7–8 months of age, 100–110 kg body weight) at a local abattoir under veterinarian control. Reproductive tracts did not display any anatomical alterations or signs of pregnancy. Ovaries were transported to the laboratory in ice-cold PBS (pH 7.4) with AAS within ~1 h of slaughter. Then healthy medium antral follicles (3–6.9 mm), characterized by a well-vascularized follicular wall and the clarity of the follicular fluid, from ovaries at an early follicular phase were manually isolated using scissors. Stage of the estrous cycle was verified by ovarian morphology and corpus luteum quality and characterized by the presence of small and medium antral follicles and corpora lutea under regression without surface vascularization or corpora albicans from the previous cycle [21].

2.3. Follicle in vitro culture

Whole ovarian follicles (n = 4/each group from different animals; a total number of ovaries used was 16) were cultured individually in a Falcon Organ Culture Dish with triangular stainless steel grid as previously described [22]. First, ovarian follicles were pre-cultured for 3 h in M199 medium supplemented with 1 % FBS and AAS. Then, experimental cultures were carried out for 12 h in fresh M199 medium with 0.1 % FBS and AAS alone (C; control) or in the presence of 1α,25$(OH)_2D_3$ (VD; 100 ng/mL) and insulin (I; 10 ng/mL) separately or in combination, VD and I (VD+I). The doses of VD and I were chosen based on literature and our previous research [6,23,24]. All cultures were maintained at 37 ℃ in a humidified atmosphere of 5 % CO_2/95 % O_2. After *in vitro* culture, follicles were fixed in 10 % neutral buffered formalin, dehydrated in an increasing gradient of ethanol, cleared in xylene and embedded in paraplast for further analyses. All *in vitro* incubations were performed in duplicates.

2.4. Hematoxylin and eosin staining

Paraplast-embedded ovarian follicles were cut into 5 μm-thick sections and mounted on 3′3′-aminopropyl-triethoxysaline-coated slides. After deparaffinization and rehydration, tissue sections were stained with hematoxylin QS for 40 s and eosin Y for 10 s. Slides were then washed in ethanol, fixed in xylene, mounted in DPX and coverslipped. Digital images were collected using a light microscope Nikon Eclipse Ni-U with a Nikon Digital DS-Fi1-U3 camera (Nikon, Tokyo, Japan) and corresponding software.

2.5. TUNEL method and quantitative analysis

Apoptotic cells were detected using the ApopTag Plus Peroxidase In Situ Apoptosis Detection Kit following the manufacturer's instruction and our previous research [25,26]. Briefly, slides were pre-treated with proteinase K solution (10 mg/mL, 15 min), immersed in 3 % H_2O_2 (10 min) and incubated in the equilibration buffer (10 min) in a humidified chamber. Next, working strength TdT enzyme was applied for 1 h at 37 °C in a dark humidified chamber and anti-digoxigenin conjugate for 30 min in a humidified chamber. Apoptotic cells were visualized by addition of 3,3′-diaminobenzidine solution. All slides were counterstained with hematoxylin QS, dehydrated through an increasing series of ethanol and mounted with DPX. A negative control was performed without the active TdT enzyme. Representative sections were photographed using a Nikon Eclipse NieU microscope and a Nikon Digital DS-Fi1-U3 camera with corresponding software.

TUNEL-positive granulosa and theca interna cells were counted across the entire follicles under light microscopy (four follicles per each examined group). The results were expressed as the percentage of apoptotic cells on the 100 cells counted within granulosa or theca interna layers, respectively [27].

2.6. FTIR spectroscopy imaging and data analysis

IR images were recorded using an Agilent 670-IR microscope coupled to a 670-IR spectrometer with 128 × 128 pixels in a focal plane array (FPA) detector. Measurements were carried out in transmission with the use of high-magnification imaging mode which provides a projected FPA pixel size of 1.1 μm × 1.1 μm giving a measured area of 141 μm × 141 μm. Three images from each sample were collected (12 images for each group in total) with 15 × Cassegrain objective and condenser optics with NA of 0.62. Regions of interest (ROIs) were chosen to cover both granular cellular and inner layers. All FTIR spectra were recorded by co-adding of 256 scans and in the range of 3800 – 900 cm^{-1} with a spectral resolution of 4 cm^{-1}.

Pre-processing of IR images and chemometric analysis were performed using CytoSpec (ver. 2.00.02), MatLab (R2015a), and Origin Pro 2022b (*v.* 9.9.5.167) software. If necessary a water vapour correction was performed on the images. Firstly, the quality of each pixel-spectrum was evaluated using the sample thickness criterion according to the intensity of the amide I band (1620–1680 cm^{-1}). After PCA-based noise reduction (15 principal components), secondary derivative FTIR spectra

were calculated with 13 smoothing points according to a Savitzky–Golay algorithm. Then, spectra were vector normalized in the region of 1000–1770 cm^{-1} to avoid clustering of the images due to the sample thickness. To extract chemical information of granulosa and theca interna cells, unsupervised hierarchical cluster analysis (UHCA) with a Ward's algorithm was performed in the region of 1000–1770 cm^{-1}. Spectral distances were computed as D-Value and the clusters were extracted according to Ward's algorithm. Then, mean second derivative spectra were calculated for both clusters. They were next used for the calculation of integral intensities of important bands or their ratios using OPUS 7.2 software. All mean spectra obtained for each group (C, VD, I, VD+I) were also averaged to one representative spectrum to evaluate spectral changes between groups and classes and presented as box charts of bands intensities or their ratios. A scheme of this imaging approach is shown in Fig. 1.

2.7. Feulgen's staining and intensity analysis

For demonstrating DNA content, ovarian follicle sections were stained with Feulgen's reaction [28,29]. Specifically, after the deparaffinization and rehydratation steps, the slides were subjected to warm (60 °C) 1 M HCl for 6 min to remove the purine bases and then to cold Schiff's reagent for 30 min. In order to stop the reaction, the specimens were washed in 10 % Na_2SO_4 (3 × 1 min). After washing with running water for 5 min, dehydration and mounting was performed.

Representative micrographs were taken using Nikon Eclipse Ni-U microscope with a Nikon Digital DS-Fi1-U3 camera and corresponding software. The intensity of DNA staining within granulosa and theca interna compartments (10 slides per each group) was examined using ImageJ software program (National Institutes of Health, Bethesda, MD, USA) and expressed as a relative optical density (ROD) following the formula: $ROD=OD_{specimen}/OD_{background}=\log(GL_{blank}/GL_{specimen})/\log(GL_{blank}=GL_{background})$, where GL is the gray level for the stained area (specimen) and the unstained area (background), and blank is the gray level measured after removing the slide from the light path [30].

2.8. Masson's trichrome staining and collagen area rate analysis

Masson's trichrome staining was used for visualization of collagen fibers. In brief, deparaffinized and rehydrated sections were treated with Weigert's iron hematoxylin for 10 min to stain the nuclei. Then, Biebrich scarlet-acid fuschin solution was applied for 7 min for collagen staining, 2.5 % phosphotungstic acid was used until the collagen loses its red color and aniline blue was utilized for 5 min to stain the collagen followed by 1 % acetic acid immersion. After washing with running water, dehydration and mounting was conducted. Representative micrographs were captured using Nikon Eclipse Ni-U microscope with a Nikon Digital DS-Fi1-U3 camera and corresponding software.

To analyze the area of positive collagen staining within theca interna, ImageJ software program was used and two-step evaluation was performed as previously described [31]. Firstly, only collagen staining area was measured in the blue channel after color deconvolution (10 slides per each group). Secondly, all the stained tissue components of the same image were measured after the conversion to 8-bit type and the

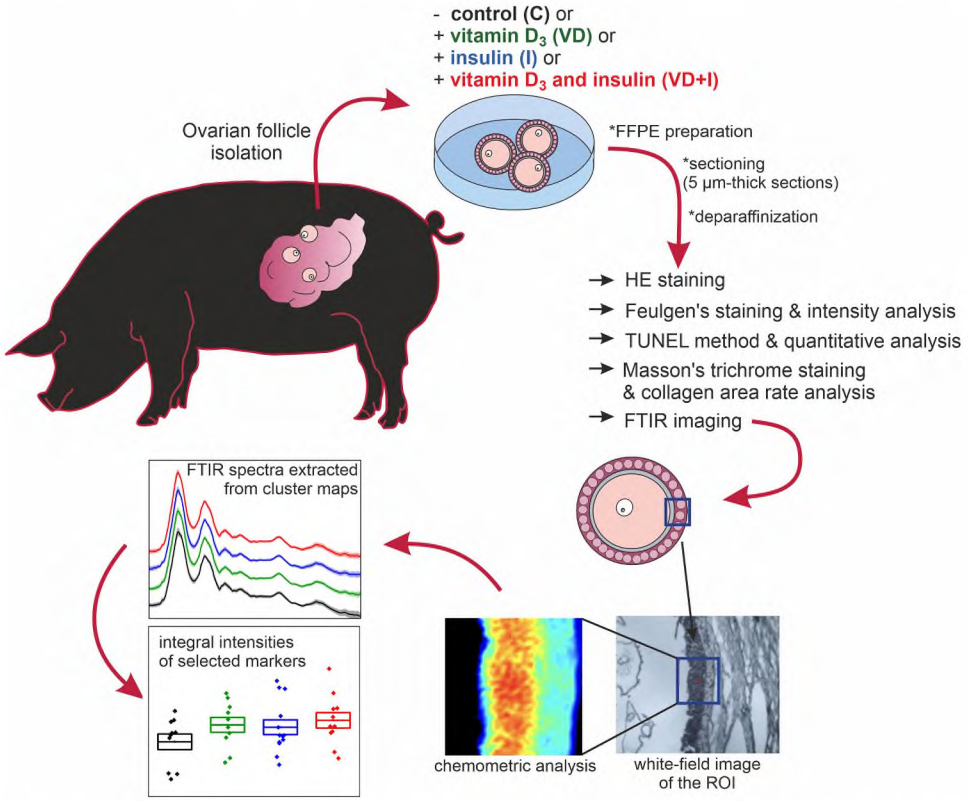

Fig. 1. A scheme of the performed experiment. Medium antral porcine ovarian follicles were *in vitro* cultured alone (C; control) or in the presence of active vitamin D_3 (VD; 100 ng/mL) and insulin (I; 10 ng/mL) separately or in combination, VD and I (VD+I). Then, formalin-fixed paraffin-embedded (FFPE) tissues were cut into 5 µm-thick sections, deparaffinized and stained with hematoxylin and eosin (H&E), Fulgen, Masson's trichrome and terminal deoxynucleotidyl transferase-mediated dUTP nick end labeling (TUNEL) methods, as well as subjected to Fourier Transform Infrared (FTIR) imaging. FTIR images were collected in selected regions of interest (ROI) including both granulosa and theca interna layers of the ovarian follicles cross-section. Spectra recorded outside the tissue area were eliminated and in the next step, chemometric analysis was performed to extract mean FTIR spectra for analyzed follicular layers from each measured ROI. All mean spectra were used to determine changes in the integral intensity of selected spectral markers and then averaged to obtain representative spectra for control (C) and treated groups (VD, I, VD+I).

threshold was applied to detect all tissue components. The final calculation of collagen area percentage was conducted following the formula: (the measured area from the first step)/(the measured area from the second step) × 100.

2.9. Statistical analysis

Statistical analysis was performed using the Statistica *v.*13.1 program (StatSoft, Inc., Tulsa, OK, USA). The data are shown as the mean ± standard error of the mean (SEM), except for FTIR data presented as mean ± standard deviation (SD). The normal distribution of data was verified by the Shapiro-Wilk test. Box plots were constructed using the statistical model (ANOVA) in the OriginPro 2022b (9.95) software for an analysis of variance. Tukey's test was employed to compute significance values p. Nonparametric Kruskal-Wallis test was used to analyze percentage of apoptotic cells, DNA staining intensity and collagen area rate. Differences were considered statistically significant at $p < 0.05$.

3. Results

3.1. Effect of vitamin D_3 and insulin alone or in combination on histology of porcine ovarian follicles

The histological analysis of porcine ovarian follicles following *in vitro* culture with VD (Fig. 2B) and I (Fig. 2C) alone or in co-treatment (VD+I) (Fig. 2D) showed normal distribution of granulosa, theca interna and externa layers as in the C group (Fig. 2A). In the C, VD and VD+I groups, there were no visible signs of follicular cells degeneration indicating lack of negative effect of either treatment or time of culture on ovarian follicle histology. Single apoptotic bodies were observed in the granulosa cells from the I group (Fig. 2C, red arrows).

3.2. Effect of vitamin D_3 and insulin alone or in combination on percentage of apoptotic cells

In situ detection of DNA fragmentation by TUNEL assay showed apoptotic cells with brown nuclei within granulosa and theca interna compartments of porcine ovarian follicles in all examined groups (Fig. 3A-D). No positive stating was observed when TdT enzyme was omitted (negative control; Fig. 3D inset). In the granulosa layer, the frequency of apoptotic cells was greater only following the I treatment (Fig. 3C) in comparison to the C, VD and VD+I groups ($p = 0.0008$, $p = 0.028$ and $p = 0.000021$, respectively), whereas there were no significant differences in the percentage of theca interna apoptotic cells between groups (Table 1).

3.3. Effect of vitamin D_3 and insulin alone or in combination on biochemical composition of porcine ovarian follicles

In order to investigate the effect of VD and I alone or in co-treatment on the total biochemical profile of porcine ovarian follicles, we employed high-definition (HD) FTIR spectroscopy imaging. Average FTIR spectra with SD of all investigated groups within granulosa and theca interna compartments are displayed in Figs. 4A and 5A, respectively. The assignment of bands to vibrations of biomolecules is presented in Table 2. Due to the removal of most lipids during the deparaffinization process with the use of xylene and ethanol, the lipid region in the FTIR spectra was not analyzed.

In the fingerprint region 1800–1000 cm^{-1} of the granulosa (Fig. 4B, C) and theca interna (Fig. 5B, C) layers, the most pronounced spectral changes were observed in the bands assigned to proteins, especially associated with alterations of their secondary structures. An increase in the 1653 cm^{-1} signal assigned to α-helices was observed in the I and VD+I groups ($p < 0.05$; Fig. 4D II) within granulosa, and in the VD and I groups ($p < 0.05$; Fig. 5D II) within theca interna compartments. These changes were accompanied by a tendency to decrease in the β-sheet contribution to the protein conformations for I and VD+I groups (box charts for the 1633 cm^{-1} band, Fig. 4D III and 5D III). Spectral variations were also observed for the bands located at 1203, 1236, and 1282 cm^{-1} specific for fibrous proteins, mainly collagens. Their semi-quantitative analysis revealed significant changes in the theca interna layer, where their greater content was found in the VD+I group than in the VD group

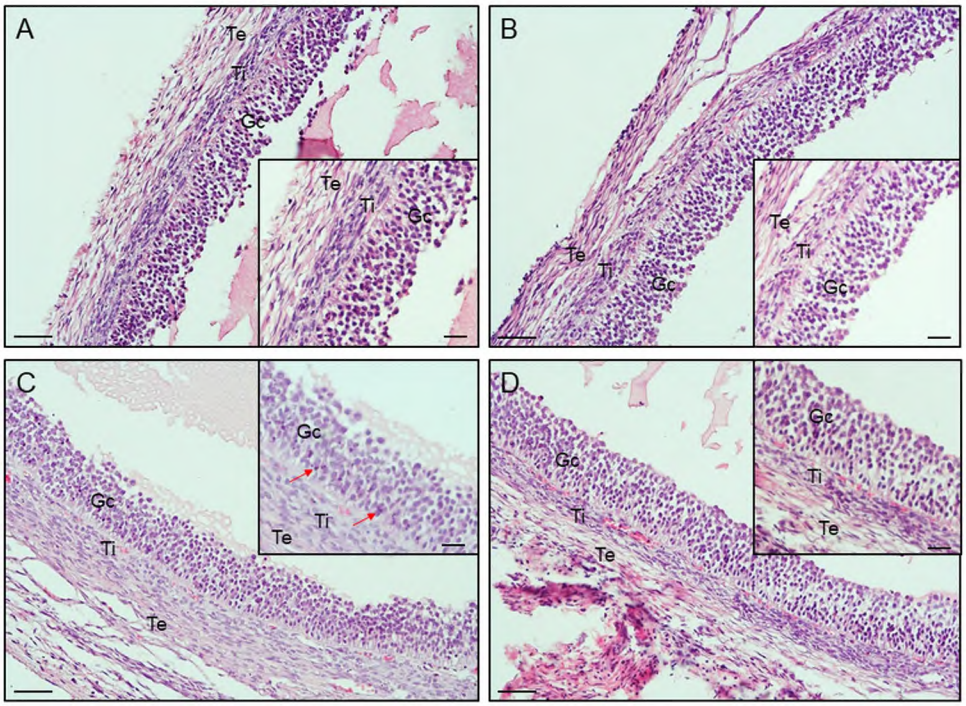

Fig. 2. Representative micrographs of hematoxylin and eosin staining of porcine ovarian follicles cultured *in vitro* from control (A), vitamin D_3 (B), insulin (C) and both vitamin D_3 and insulin (D) treated groups. Scale bar = 50 μm (A, B, C, D) or 25 μm (all insets). Gc – granulosa cells; Ti – theca interna cells; Te – theca externa cells; red arrows – apoptotic bodies.

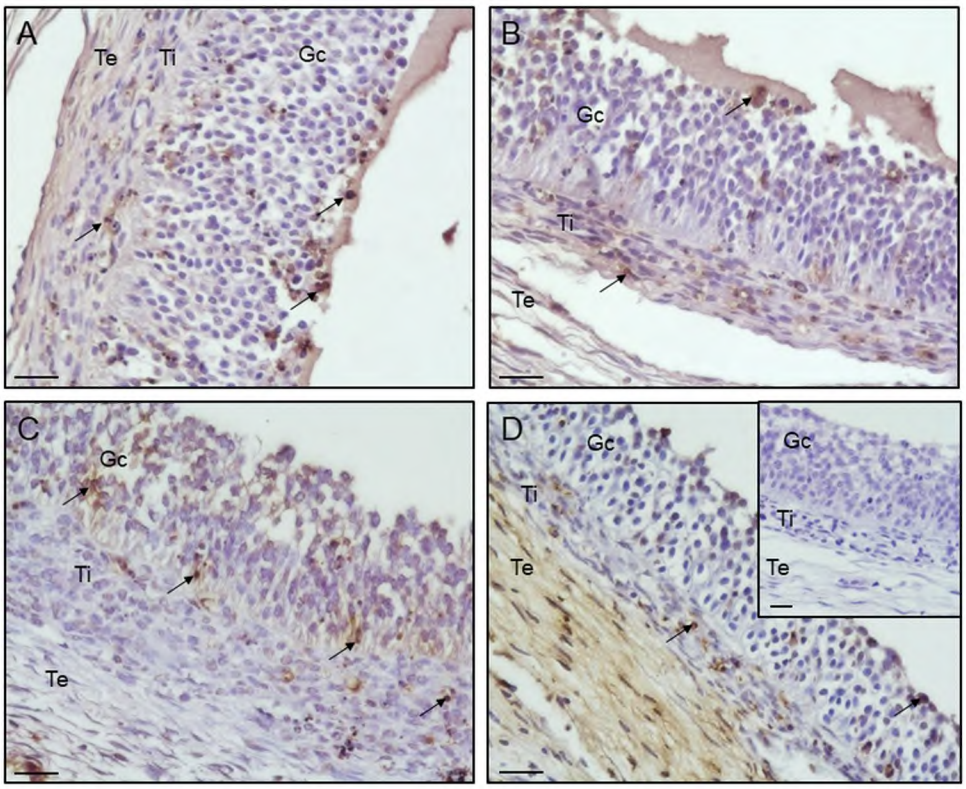

Fig. 3. Representative micrographs of *in situ* detection of apoptotic cells in porcine ovarian follicles cultured *in vitro* from control (A), vitamin D_3 (B), insulin (C) and both vitamin D_3 and insulin (D) treated groups. Apoptotic cells were identified using TUNEL assay. Arrows indicate apoptotic cells. A negative control was performed without active TdT enzyme (D, inset). Scale bar = 25 μm (A, B, C, D). Gc – granulosa cells; Ti – theca interna cells; Te – theca externa cells.

Table 1
Effect of vitamin D_3 and insulin alone or in combination on percentage (%) of apoptotic cells and intensity of Feulgen staining (ROD; relative optical density) within granulosa and theca interna layers, as well as collagen area rate (%) within theca interna of porcine ovarian follicles cultured *in vitro*. Results are expressed as mean ± standard error mean (SEM). Different letter superscripts indicate significant differences between groups (Kruskal-Wallis test; $p < 0.05$).

		Groups (n = 4)			
		Control (C)	Vitamin D_3 (VD)	Insulin (I)	Vitamin D_3 + insulin (VD+I)
Percentage (%) of apoptotic cells	Granulosa	0.92 ± 0.29^{a}	1.41 ± 0.29^{a}	5.5 ± 0.88^{b}	0.5 ± 0.23^{a}
	Theca interna	2.33 ± 0.45^{a}	2.66 ± 0.56^{a}	1.25 ± 0.38^{a}	0.92 ± 0.28^{a}
Feulgen staining intensity (ROD)	Granulosa	0.78 ± 0.04^{a}	0.71 ± 0.04$^{a, c}$	0.69 ± 0.66$^{a, c}$	0.57 ± 0.04$^{b, c}$
	Theca interna	0.78 ± 0.03^{a}	0.66 ± 0.06$^{a, c}$	0.64 ± 0.04$^{a, c}$	0.51 ± 0.05$^{b, c}$
Collagen area (%)	Theca interna	40.88 ± 2.41^{a}	23.5 ± 2.64^{b}	40.63 ± 2.43^{a}	44.37 ± 2.98^{a}

($p < 0.05$; Fig. 5D IV). It seems that VD and I applied individually induced the decomposition of fibrous proteins compared to the control (Fig. 5D IV). Considering the total level of proteins that show the tendency to decrease in both layers in the VD and I groups compared to C and VD+I, we rather suggest a remodeling process of proteins than the synthesis of new ones (Fig. 4D I and 5D I).

The content of nucleic acids was not significantly affected by the treatment (Fig. 4D V,VI and 5D V,VI). Both RNA and DNA slightly decreased in the granulosa of the VD+I group, while a considerable synthesis of RNA and lowering DNA content were observed in theca interna layer of the ovarian follicle.

For the sugar classes, the FTIR spectra did not exhibit the alternations of polysaccharides and glycoproteins (signals at 1170 and 1059 cm^{-1}), but we observed a variation in the content of monosaccharides (signal at 1030 cm^{-1}). Namely, monosaccharides were only synthesized in the granulosa layer due to the treatment by VD+I (Fig. 4C), whereas only VD did not cause their production in the theca interna compartment (Fig. 5C).

3.4. *Effect of vitamin D_3 and insulin alone or in combination on DNA content*

DNA of granulosa and theca interna cells was stained positively magenta using Feulgen's reaction in all examined groups (Fig. 6A-D). The DNA content expressed as staining intensity was markedly reduced in the VD+I group (Fig. 6D) when compared to the C group (Fig. 6A) either in granulosa ($p = 0.01$) or theca interna ($p = 0.0018$) cells (Table 1).

3.5. *Effect of vitamin D_3 and insulin alone or in combination on collagen area rate*

In all studied groups, the blue color collagen staining was observed within theca interna and externa layers, as well as basal lamina of porcine ovarian follicles (Fig. 7A-D). The analysis of positive staining area in theca interna layer shows its lower percentage in the VD group (Fig. 7B) than in the C (Fig. 7A), I (Fig. 7C), and VD+I (Fig. 7D) groups ($p = 0.02$, $p = 0.03$ and $p = 0.002$, respectively; Table 1).

4. Discussion

The present study investigated for the first time the effect of vitamin D_3 and insulin alone or in combination on biomolecular composition of granulosa and theca interna layers of porcine ovarian follicles using

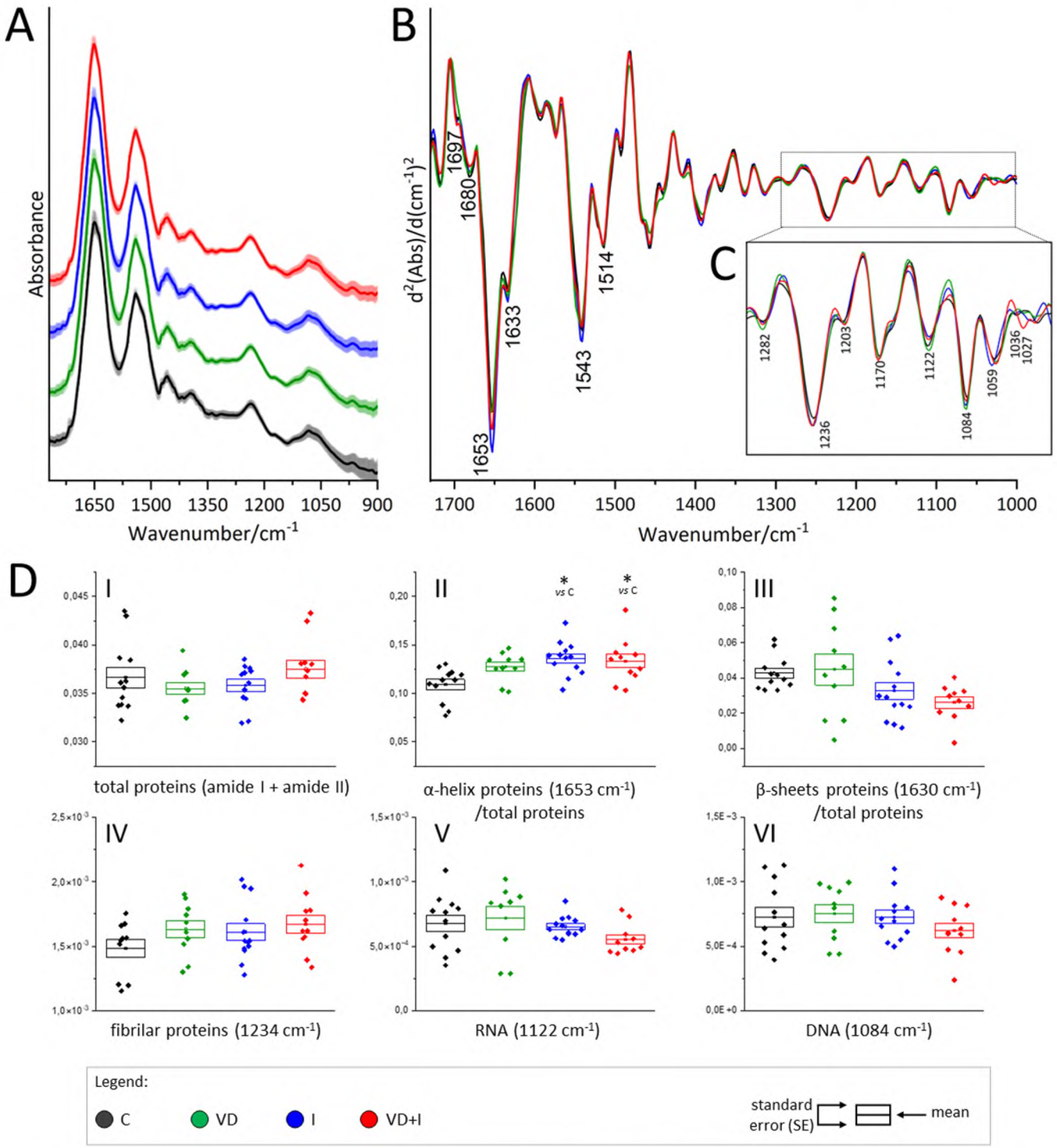

Fig. 4. Average FTIR spectra with standard deviation (SD, shading) of the granulosa layer of porcine ovarian follicles cultured *in vitro* from control (C), vitamin D_3 (VD), insulin (I), and both vitamin D_3 and insulin (VD+I) treated groups (A), their second derivative spectra in the region of 1710–1480 (B), and 1300–1000 cm^{-1} (C), and changes in content of the selected biocomponents (D). *$p < 0.05$, one-way ANOVA with *post hoc* Tukey's test.

FTIR spectroscopy. Combining this technique with common histological staining methods, we revealed pronounced changes in the content of fibrous proteins (mainly collagens) within theca interna following vitamin D_3 and insulin co-administration. Treatment-dependent differences were also observed in the secondary structure of proteins, DNA content and monosaccharides production in both follicular compartments. Based on our FTIR findings, it is possible to attribute the observed alterations to biological processes that could be regulated by vitamin D_3 and insulin in the ovarian follicle.

Herein, we have firstly performed histological assessment of the ovarian follicles after *in vitro* incubation. In all examined groups, the follicles displayed the proper organization with visible granulosa and theca layers. Time of *in vitro* culture did not affect ovarian follicle's wall histology and did not induce atresia as shown in the control group, consitently with previous report on pigs [22]. Noteworthy, insulin treatment slightly increased the percentage of apoptotic cells within

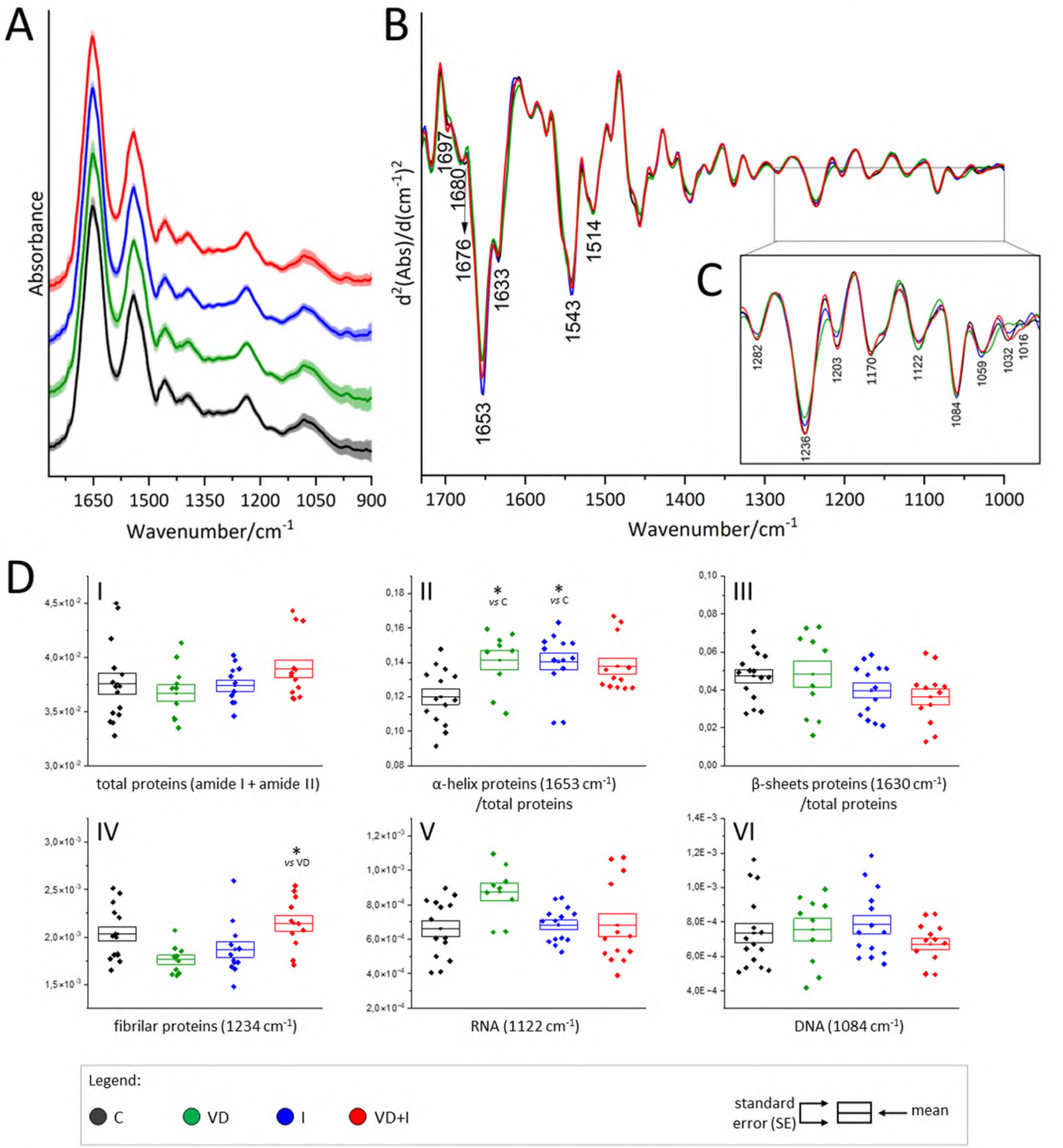

Fig. 5. Average FTIR spectra with standard deviation (SD, shading) of the theca interna layer of porcine ovarian follicles cultured *in vitro* from control (C), vitamin D_3 (VD), insulin (I), and both vitamin D_3 and insulin (VD+I) treated groups (A), their second derivative spectra in the region 1710–1480 (B), and 1300–1000 cm^{-1} (C), and changes in content of the selected biocomponents (D). *$p < 0.05$, one-way ANOVA with *post hoc* Tukey's test.

granulosa layer compared to other groups that was confirmed by TUNEL assay. Likewise, high concentration of insulin used to mimic insulin resistance promoted apoptosis in rat granulosa cells, suggesting its role in the pathogenesis of PCOS [35].

Proteins are important molecules of each living cell and play a vital role in all physiological processes. Predominant ovarian functions, namely folliculogenesis and steroidogenesis, are regulated by hormones, growth factors and enzymes, which are proteins [36]. Therefore, spectral analysis of protein content in follicular cells could provide an information about their physiological state. In the present research, the total protein abundance within granulosa and theca interna layers was unchanged among examined groups, however differences in the secondary structure were noted. We have found an increased band intensity at 1653 cm^{-1} assigned to α-helical conformation of proteins; in the granulosa cells, this effect was observed in the I and VD+I groups, while within theca interna, in the VD and I once. In those groups, the

Table 2
Positions of bands observed in second derivative FTIR spectra with their assignments to biocomponents [32–34].

IR band position/ cm^{-1}	Assignment
1697	Amide I: antiparallel β-sheet conformation in proteins
1681,1676	Amide I: turns, loops in proteins
1653	Amide I; α-helices in proteins
1633	Amide I: β-sheets in proteins
1543	Amide II: proteins
1514	In-plane deformation vibration C-H of phenyl ring: tyrosine residues
1282, 1236, 1203	Amide III: fibrous proteins (mainly collagen)
1170	symmetric stretching vibrations of -CO-O-C polysaccharides, glycoproteins
1122	Stretching vibrations of C-O of ribose ring: RNA
1084	symmetric stretching vibrations of PO_2^- group: DNA
1059	Stretching vibrations of -CO-O-C; polysaccharides
1030	Deformation vibration of C-OH: monosaccharides

decreasing tendency in the band intensity at 1633 cm^{-1} attributed to β-sheet was noticed, suggesting enhanced conversion to α-helices in the secondary structure of proteins. In the ovary, spectral changes in the range reflected secondary structure of proteins were presented by this time in the research on ovarian tumor [37,38], showing a shift to β-sheet in cancerous tissue. In addition, the conversion from α-helix to β-strand might induce amyloidogenic proteins to self-assemble into fibrils causing fatal diseases *e.g.* prion diseases [39]. Along this line, it appears that protein structural conversion to α-helices observed herein might be a molecular marker of rather beneficial vitamin D_3 and insulin action within the ovarian follicle. Indeed, both examined factors were recognized as positive regulators of follicle development and steroids synthesis in the ovary [1,5,40].

In this study, another spectral alterations were observed in bands intensities at 1203, 1236, and 1282 cm^{-1} specific for fibrous proteins, mainly collagens; co-treatment of vitamin D_3 and insulin resulted in their increased abundance in theca interna layer when compared to the VD group. Following Massons's trichrome staining, greater collagen area within theca interna was noted in the VD+I, I and C groups than in the VD group. These discrepancies might be due to the fact that FTIR results are related to spectral region assigned overall to fibrous proteins, whereas Massons's trichrome stains only collagens. In the porcine ovarian follicles, prominent collagen expression was examined in the theca compartment and basal lamina with no positive staining in the granulosa layer [41], consistently with our current outcomes. Different collagen types play crucial role in follicle development, basement membrane formation, steroidogenesis and ovulation [42]. On the other hand, excessive accumulation of collagen occurs during ovarian aging or PCOS [43,44], leading to ovarian stiffness. It seems that vitamin D_3 and insulin interactions might be important for fibrous protein remodeling within theca interna compartment, modulating thereby ovarian follicle functions.

Besides proteins, nucleic acids are an indispensable element of each cell. Although we have not found significant spectral alterations in the region specific to either RNA or DNA, some tendency to lower DNA content within granulosa and theca interna layers in the VD+I group was noticed. That was further confirmed by the analysis of Fulgen's staining intensity, showing decreased DNA content in the VD+I group when compared to the C group in both follicular compartments. These results indicate attenuated proliferative activity of granulosa and theca interna cells in response to vitamin D_3 and insulin co-administration. Both agents acting separately were shown to have predominantly a dose-dependent stimulatory effect on ovarian cells proliferation [5,40]. Herein, utilized doses of vitamin D_3 and insulin alone did not increased DNA content, but their co-treatment induced the opposite effect, suggesting possible mutual inhibition.

A detailed analysis of the spectral range assigned to carbohydrates distinguished a characteristic trend of alterations of the band at

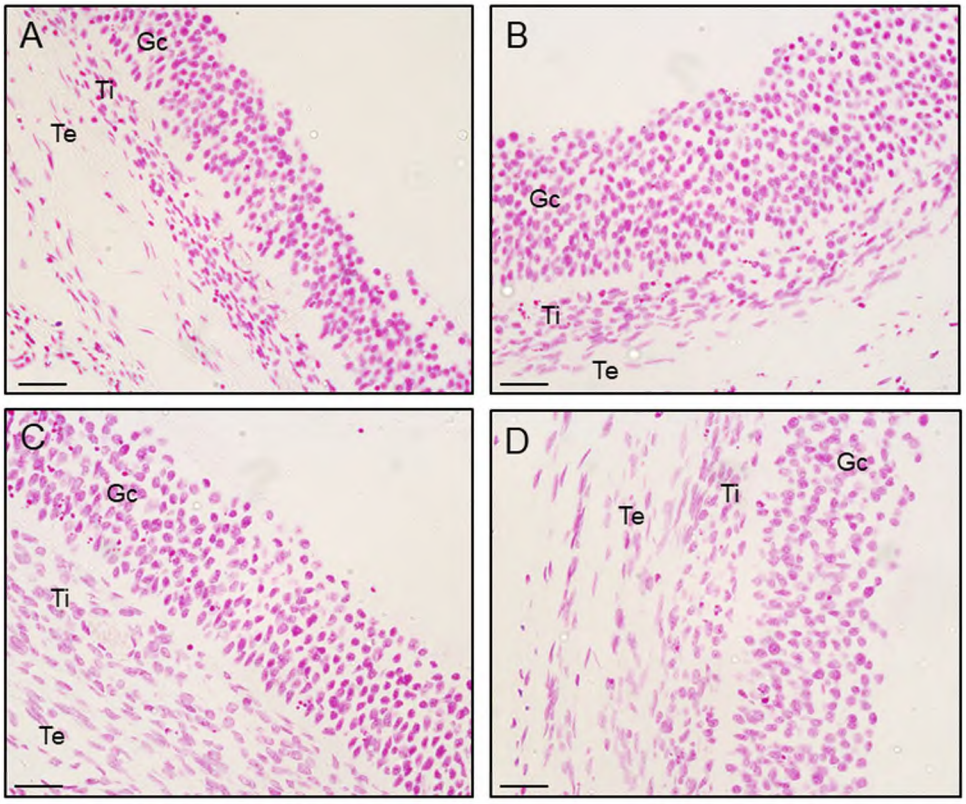

Fig. 6. Representative micrographs of Feulgen's staining of porcine ovarian follicles cultured *in vitro* from control (A), vitamin D_3 (B), insulin (C) and both vitamin D_3 and insulin (D) treated groups. Scale bar = 25 μm (A, B, C, D). Gc – granulosa cells; Ti – theca interna cells; Te – theca externa cells.

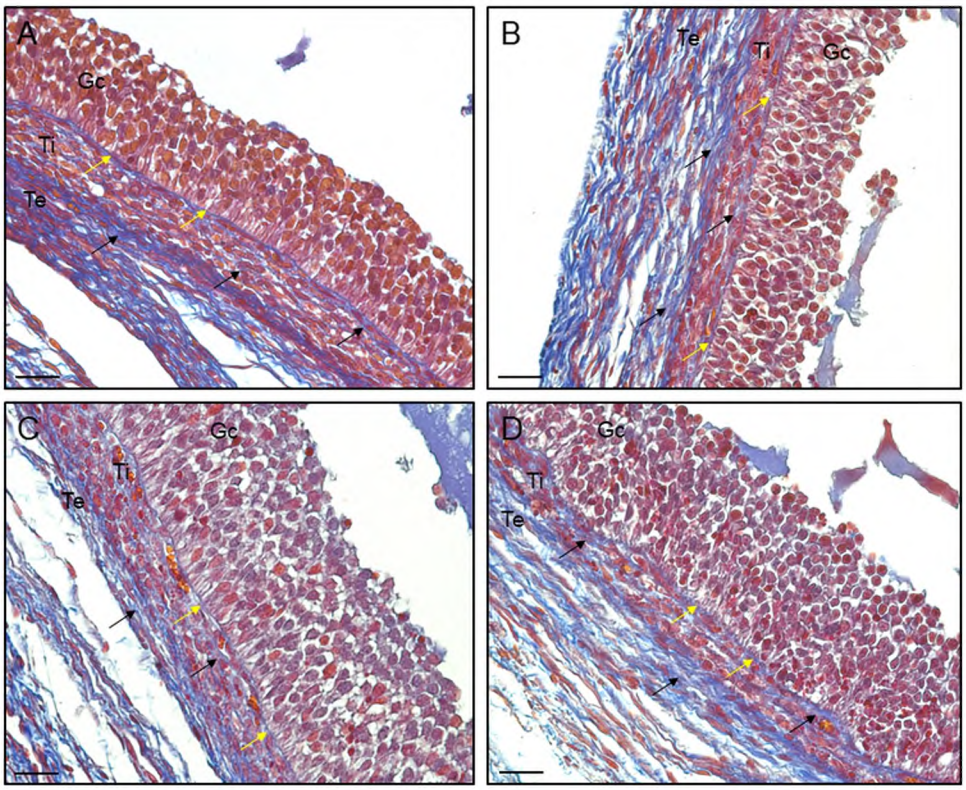

Fig. 7. Representative micrographs of Masson's trichrome staining of porcine ovarian follicles cultured *in vitro* from control (A), vitamin D_3 (B), insulin (C) and both vitamin D_3 and insulin (D) treated groups. Black arrows indicate positive blue staining of collagen fibers within theca compartment, while yellow arrows in basal lamina. Scale bar = 25 μm (A, B, C, D). Gc – granulosa cells; Ti – theca interna cells; Te – theca externa cells.

1030 cm^{-1} that originates from the C—OH stretching mode and is a spectral marker of monosaccharides. In the granulosa layer, only the VD+I group synthesized monosaccharides, while within theca interna compartment their production was found in the C, I and VD+I group, suggesting activation of different metabolic pathways of sugar biosynthesis, especially after vitamin D_3 and insulin co-administration in ovarian cells. Further analyses are required to reveal which specific monosaccharides undergo alterations induced by vitamin D_3 and insulin.

5. Conclusion

In conclusion, significant changes observed in the spectra assigned to fibrous proteins, secondary structure of proteins, DNA and monosaccharides within porcine ovarian follicle compartments could be consider as molecular markers of the physiological status of ovarian cells following vitamin D_3 and insulin action/interaction. In particular, they could be indicators for further specific staining and proteomic/metabolomic studies. Although FTIR-based examination of induced changes in molecular composition of porcine ovarian follicle layers needs additional studies to validate our observations, it seems to be a potential tool in prediction of functional changes within granulosa and theca interna cells. Thereby the route of vitamin D_3 and insulin action within the ovary could be determined that might be powerful approach considering various ovarian pathologies attributed to disturbed vitamin D_3 and insulin levels. Thus, FTIR spectroscopy could join the group of common techniques used in ovary-oriented studies.

Ethical approval

The use of animals was in accordance with the Act of 15 of January 2015 on the Protection of Animals Used for Scientific or Educational Purposes and Directive 2010/63/EU of the European Parliament and the Council of 22 of September 2010 on the protection of animals used for scientific purposes.

Funding

This study was partly supported by a grant from the National Science Centre (NCN, Poland, grant no. 2019/35/O/NZ9/02678 to MG).

CRediT authorship contribution statement

K.K.: Conceptualization, Investigation, Methodology, Visualization, Writing - Original Draft. E.W.: Investigation, Methodology, Formal analysis, Visualization, Writing - Original Draft. K.M.: Methodology, Writing - Review & Editing. M.G.: Conceptualization, Methodology, Writing - Original Draft, Writing - Review & Editing, Supervision, Funding acquisition. All authors read and approved the final manuscript.

Declaration of Competing Interest

The authors declare that they have no known competing financial interests or personal relationships that could have appeared to influence the work reported in this paper. No potential conflict of interests relevant to this article were reported.

Acknowledgments

We would like to thank Dagmara Podkowa, PhD (Department of Comparative Anatomy, Institute of Zoology and Biomedical Research, Jagiellonian University, Krakow, Poland) for the possibility to perform Masson's trichrome staining.

References

[1] Grzesiak M. Vitamin D_3 action within the ovary - an updated review. Physiol Res 2020;69(3):371–8.
[2] Xu F, Wolf S, Green O, Xu J. Vitamin D in follicular development and oocyte maturation. Reproduction 2021;161(6):R129–37.
[3] Grzeczka A, Graczyk S, Skowronska A, Skowronski MT, Kordowitzki P. Relevance of vitamin D and its deficiency for the ovarian follicle and the oocyte: an update. Nutrients 2022;14(18):3712.
[4] Merhi Z, Doswell A, Krebs K, Cipolla M. Vitamin D alters genes involved in follicular development and steroidogenesis in human cumulus granulosa cells. J Clin Endocrinol Metab 2014;99(6):E1137–45.
[5] Grzesiak M, Tchurzyk M, Socha M, Sechman A, Hrabia A. An overview of the current known and unknown roles of vitamin D_3 in the female reproductive system: lessons from farm animals, birds, and fish. Int J Mol Sci 2022;23(22):14137.
[6] Grzesiak M, Knapczyk-Stwora K, Slomczynska M. Vitamin D_3 in ovarian antral follicles of mature gilts: Expression of its receptors and metabolic enzymes, concentration in follicular fluid and effect on steroid secretion *in vitro*. Theriogenology 2021;160:151–60.
[7] Cashman KD. Global differences in vitamin D status and dietary intake: a review of the data. Endocr Connect 2022;11(1):e210282.
[8] Shahrokhi SZ, Ghaffari F, Kazerouni F. Role of vitamin D in female reproduction. Clin Chim Acta 2016;455:33–8 (doi).
[9] Dovnik A, Dovnik NF. Vitamin D and ovarian cancer: systematic review of the literature with a focus on molecular mechanisms. Cells 2020;9(2):335.
[10] Kaminska K, Grzesiak M. The relationship between vitamin D_3 and insulin in polycystic ovary syndrome - a critical review. J Physiol Pharm 2021;72(1):13–22.
[11] Kalyanaraman R, Pal L. A narrative review of current understanding of the pathophysiology of polycystic ovary syndrome: focus on plausible relevance of vitamin D. Int J Mol Sci 2021;22(9):4905.
[12] Grzesiak M, Burzawa G, Kurowska P, Blaszczyk K, Szlaga A, Blasiak A, Sechman A, Rak A. Altered vitamin D_3 metabolism in the ovary and periovarian adipose tissue of rats with letrozole-induced PCOS. Histochem Cell Biol 2021;155(1):101–16.
[13] Baker MJ, Trevisan J, Bassan P, Bhargava R, Butler HJ, Dorling KM, Fielden PR, Fogarty SW, Fullwood NJ, Heys KA, Hughes C, Lasch P, Martin-Hirsch PL, Obinaju B, Sockalingum GD, Sulé-Suso J, Strong RJ, Walsh MJ, Wood BR, Gardner P, Martin FL. Using Fourier transform IR spectroscopy to analyze biological materials. Nat Protoc 2014;9(8):1771–91.
[14] Sahu R, Mordechai S. Fourier transform infrared spectroscopy in cancer detection. Future Oncol 2005;1(5):635–47.
[15] Zadka Ł, Chrabaszcz K, Buzalewicz I, Wiercigroch E, Glatzel-Plucińska N, Szleszkowski Ł, Gomułkiewicz A, Piotrowska A, Kurnol K, Dzięgiel P, Jurek T, Malek K. Molecular profiling of the intestinal mucosa and immune cells of the colon by multi-parametric histological techniques. Sci Rep 2021;11(1):11309.
[16] Augustyniak K, Chrabaszcz K, Smeda M, Stojak M, Marzec KM, Malek K. High-resolution Fourier Transform Infrared (FT-IR) spectroscopic imaging for detection of lung structures and cancer-related abnormalities in a murine model. Appl Spectrosc 2022;76(4):439–50.
[17] Kujdowicz M, Perez-Guaita D, Chlosta P, Okon K, Malek K. Evaluation of grade and invasiveness of bladder urothelial carcinoma using infrared imaging and machine learning. Analyst 2023;148(2):278–85.
[18] Li L, Wu J, Yang L, Wang H, Xu Y, Shen K. Fourier transform infrared spectroscopy: an innovative method for the diagnosis of ovarian cancer. Cancer Manag Res 2021;13:2389–99.
[19] Bendixen E, Danielsen M, Larsen K, Bendixen C. Advances in porcine genomics - a toolbox for developing the pig as a model organism for molecular biomedical research. Brief Funct Genom 2010;9(3):208–19.
[20] Kuzmuk KN, Schook LB. Pig as a model for biomedical sciences. In: Rothschild MF, Ruvinsky A, editors. The genetics of the pig. CABI Publishing; 2011. p. 426–44.
[21] Akins EL, Morrisette MC. Gross ovarian changes during estrus cycle of swine. Am J Vet Res 1968;29(10):1953–7.
[22] Duda M, Grzesiak M, Knet M, Knapczyk-Stwora K, Tabarowski Z, Michna A, Slomczynska M. The impact of antiandrogen 2-hydroxyflutamide on the expression of steroidogenic enzymes in cultured porcine ovarian follicles. Mol Biol Rep 2014;41(7):4213–22.
[23] Rice S, Pellatt LJ, Bryan SJ, Whitehead SA, Mason HD. Action of metformin on the insulin-signaling pathway and on glucose transport in human granulosa cells. J Clin Endocrinol Metab 2011;96(3):E427–35.
[24] Smolikova K, Mlynarcikova A, Scsukova S. Effect of 1α,25-dihydroxyvitamin D3 on progesterone secretion by porcine ovarian granulosa cells. Endocr Regul 2013;47(3):123–31.
[25] Grzesiak M, Knapczyk-Stwora K, Slomczynska M. Induction of autophagy in the porcine corpus luteum of pregnancy following anti-androgen treatment. J Physiol Pharm 2016;67(6):933–42.
[26] Grzesiak M, Kapusta K, Kaminska K, Palka S, Kmiecik M, Zubel-Lojek J. Effect of dietary supplementation with nettle or fenugreek on folliculogenesis and steroidogenesis in the rabbit ovary - an in vivo study. Theriogenology 2021;173:1–11.
[27] Durlej M, Knapczyk-Stwora K, Slomczynska M. Prenatal and neonatal flutamide administration increases proliferation and reduces apoptosis in large antral follicles of adult pigs. Anim Reprod Sci 2012;132(1–2):58–65.
[28] Leśniak-Walentyn A, Hrabia A. Expression and localization of matrix metalloproteinases (MMP-2, -7, -9) and their tissue inhibitors (TIMP-2, -3) in the chicken oviduct during pause in laying induced by tamoxifen. Theriogenology 2017;88:50–60.
[29] Kobayashi S, Saio M, Fukuda T, Kimura K, Hirato J, Oyama T. Image analysis of the nuclear characteristics of emerin protein and the correlation with nuclear grooves and intranuclear cytoplasmic inclusions in lung adenocarcinoma. Oncol Rep 2019;41(1):133–42.
[30] Smolen AJ. Image analytic techniques for quantification of immunocytochemical staining in the nervous system. In: Conn PM, editor. Methods in neurosciences. New York: Academic Press; 1990. p. 208–29.
[31] Ersoy Canillioglu Y, Senturk GE, Sahin H, Sahin S, Seval-Celik Y. The distribution of Foxp3 and CD68 in preeclamptic and healthy placentas: a histomorphological evaluation. J Histochem Cytochem 2023;71(4):211–25.
[32] Belbachir K, Noreen R, Gouspillou G, Petibois C. Collagen types analysis and differentiation by FTIR spectroscopy. Anal Bioanal Chem 2009;395(3):829–37.
[33] Staniszewska E, Malek K, Baranska M. Rapid approach to analyze biochemical variation in rat organs by ATR FTIR spectroscopy. Spectrochim Acta A Mol Biomol Spectrosc 2014;118:981–6.
[34] Lu R, Li WW, Katzir A, Raichlin Y, Mizaikoff B, Yu HQ. Fourier transform infrared spectroscopy on external perturbations inducing secondary structure changes of hemoglobin. Analyst 2016;141(21):6061–7.
[35] Ni XR, Sun ZJ, Hu GH, Wang RH. High concentration of insulin promotes apoptosis of primary cultured rat ovarian granulosa cells via its increase in extracellular HMGB1. Reprod Sci 2015;22(3):271–7.
[36] Monget P, McNatty K, Monniaux D. The crazy ovary. Genes (Basel) 2021;12(6):928.
[37] Mehrotra R, Tyagi G, Jangir DK, Dawar R, Gupta N. Analysis of ovarian tumor pathology by fourier transform infrared spectroscopy. J Ovarian Res 2010;3:27.
[38] Lei L, Bi X, Sun H, Liu S, Yu M, Zhang Y, Weng S, Yang L, Bao Y, Wu J, Xu Y, Shen K. Characterization of ovarian cancer cells and tissues by Fourier transform infrared spectroscopy. J Ovarian Res 2018;11(1):64.
[39] Yang WZ, Ko TP, Corselli L, Johnson RC, Yuan HS. Conversion of a beta-strand to an alpha-helix induced by a single-site mutation observed in the crystal structure of Fis mutant Pro26Ala. Protein Sci 1998;7(9):1875–83.
[40] Dupont J, Scaramuzzi RJ. Insulin signalling and glucose transport in the ovary and ovarian function during the ovarian cycle. Biochem J 2016;473(11):1483–501.
[41] Parkes WS, Amargant F, Zhou LT, Villanueva CE, Duncan FE, Pritchard MT. Hyaluronan and collagen are prominent extracellular matrix components in bovine and porcine ovaries. Genes (Basel) 2021;12(8):1186.
[42] Berkholtz CB, Lai BE, Woodruff TK, Shea LD. Distribution of extracellular matrix proteins type I collagen, type IV collagen, fibronectin, and laminin in mouse folliculogenesis. Histochem Cell Biol 2006;126(5):583–92.
[43] Amargant F, Manuel SL, Tu Q, Parkes WS, Rivas F, Zhou LT, Rowley JE, Villanueva CE, Hornick JE, Shekhawat GS, Wei JJ, Pavone ME, Hall AR, Pritchard MT, Duncan FE. Ovarian stiffness increases with age in the mammalian ovary and depends on collagen and hyaluronan matrices. Aging Cell 2020;19(11):e13259.
[44] Wood CD, Vijayvergia M, Miller FH, Carroll T, Fasanati C, Shea LD, Brinson LC, Woodruff TK. Multi-modal magnetic resonance elastography for noninvasive assessment of ovarian tissue rigidity in vivo. Acta Biomater 2015;13:295–300.